Applicability of seawater as a mixing and curing agent in 4-year-old concrete

Dasar, Amry
Department of Civil Engineering, Universitas Sulawesi Barat

パタ, ダリア
Department of Civil Engineering, Universitas Sulawesi Barat

濱田, 秀則
九州大学大学院工学研究院社会基盤部門

Sagawa, Yasutaka
九州大学大学院工学研究院社会基盤部門

他

出版情報：Construction and Building Materials. 259 (119692), 2020-10-30. Elsevier
バージョン：
権利関係：

Applicability of seawater as a mixing and curing agent in 4-year-old concrete

Amry Dasar[a*], Dahlia Patah[a], Hidenori Hamada[b], Yasutaka Sagawa[b] and Daisuke Yamamoto[b]

[a]Department of Civil Engineering, Universitas Sulawesi Barat, Jl. Prof. Dr. Baharuddin Lopa, S.H., Lingkungan Talumung, West Sulawesi Province, Majene 91214, Indonesia (Former Doctoral Student, Graduate School of Engineering, Department of Civil and Structural Engineering, Kyushu University, 744 Motooka, Nishi-ku, Fukuoka 819-0395, Japan)

[b]Department of Civil and Structural Engineering, Kyushu University, 744 Motooka, Nishi-ku, Fukuoka 819-0395, Japan

* Corresponding author. Tel.: +62-823-4971-0201; E-mail address: amry.dasar@unsulbar.ac.id; amrydasar@gmail.com

ABSTRACT

In this study, the applicability of seawater as mixing and curing water in 4-year-old mortar cement specimens is evaluated. In certain scenarios, seawater might be the only agent available, and hence, it is necessary to optimize conditions for its application in concrete structures. Unlike in previous studies, we focused on evaluating the long-term

performance of reinforced mortar specimens exposed to seawater. The specimens comprise ordinary Portland cement (OPC) and supplementary cementitious materials (SCMs) as well as reinforced with plain steel, epoxy-coated, or stainless steel bars. The fabricated specimens were subjected to wetting-drying cycles (mimicked for tidal/splash zones) in the laboratory and corrosion was evaluated by electrochemical techniques. Seawater can be employed as a mixing and curing agent if proper concrete design is conducted. Further, SCMs exhibited better performance than OPC; similarly, epoxy-coated and stainless steel bars exhibited better corrosion resistance than plain steel bars. The results obtained in this study highlight the need to study the application of seawater in concrete mixing.

KEYWORDS:

Seawater mixing; corrosion; electrochemical methods; supplementary cementitious materials; epoxy-coated bars; stainless steel bars; chloride content

1. INTRODUCTION

Engineers commonly believe that seawater is not suitable for use in concrete, particularly in concrete embedded with reinforcing bars as it may lead to corrosion [1]. Meanwhile, freshwater (tap water) depletion is progressing at a rapid pace globally [2, 3]. Therefore, it is becoming imperative to use seawater in concrete production because tap-

water reserves are either limited or its transport is costly. Such conditions are often encountered in coastal projects and construction engineers are then beset with doubts about the advisability of using seawater. However, in unavoidable situations, the use of seawater is recommended for plain concrete [4, 5].

There are several reports available on the applicability of seawater in concrete [6-11]. In most of these studies, researchers focused on the workability and strength performance of concrete made with seawater, particularly in the early ages. The workability of seawater-mixed concrete (i.e., concrete with seawater mixing instead of tap water) has not attracted as much attention as sea sand concrete [7, 12, 13]. Katano [7] reported that the initial and final setting times of seawater concrete were shorter by 90 and 135 min, respectively, than those of tap-water-mixed concrete. In addition, most experiments on the strength performance of seawater concrete indicated a higher early-age strength when compared to tap-water-mixed concrete [6, 9, 14, 15]. Narver [16, 17] and Otsuki [17] reported that the long-term compressive strength of seawater concrete was either inferior or slightly higher than that of ordinary concrete. However, there is not much information on the corrosion behavior of reinforcing bars in seawater concrete, which is necessary to use seawater as a mixing and curing agent for concrete.

Currently, researchers are intent on analyzing the applicability of seawater in concrete, especially to understand how to deal with the associated corrosion risks. Mohammed et al. [6] found that using seawater instead of tap-water in reinforced cylindrical concrete

specimens exposed to a tidal environment for 15 years resulted in a large number of corrosion pits and greater pit depth on steel bars. Shalon and Rapheal observed serious corrosion in steel bars embedded in concrete specimens exposed to moist air [18]. Other studies also confirmed the high vulnerability of reinforcing bars to corrosion when seawater was used as the mixing agent [19].

In the previous literature [6, 18, 19] reported that seawater as a mixing and curing agent obviously lead to the serious corrosion of steel bars embedded in concrete. Therefore, this study proposed the method that seawater can be employed as a mixing and curing agent. In this study, mortar specimens were cast with seawater using ordinary fine aggregate (desalted/washed sea sand) [20-23]. The present study focuses on the effect of seawater, rather than sea sand, on the corrosion activity of steel bars embedded in concrete. Mortar specimens were made with ordinary Portland cement (OPC) and supplementary cementitious materials (SCMs) with ground granulated blast furnace slag (GGBFS) with a surface area of 4000 cm^2/g. Three types of reinforcing bars, namely plain bars (PS), epoxy-coated bars (EC), and stainless steel bars (SS), were used in this evaluation. Their corrosion behavior was exhaustively evaluated over a 4-year period in laboratory conditions with confined rooms using electrochemical methods. It is considered that a proper concrete design (i.e., sufficient concrete cover and low water to binder (W/B) ratio) is necessary to increase the usability of seawater in concrete. Further, GGBFS (SCMs) increase the corrosion resistance of the embedded reinforcement while epoxy-coated and

stainless steel bars exhibit good corrosion resistance. Studying the effect of seawater on degree of corrosion will provide information for improving the usability of seawater in concrete, which is the major aim of this study.

2. MATERIALS AND METHODS

2.1 Materials

Mortar specimens were mixed with either tap water or seawater. They were fabricated with OPC, SCMs, and GGBFS. The physical properties and chemical compositions of the materials are shown in **Table 1** while the chemical composition of natural seawater is shown in **Table 2**. Seawater used for mixing and curing was directly taken from a natural sea environment in the south-west of Japan (see **Fig. 1**).

Table 1. Physical properties and chemical composition of materials

Description	OPC	GGBFS	Sand
Physical Properties			
Density, g/cm³	3.16	2.91	2.58
Fineness Modulus (F.M)	-	-	2.77
Chemical Composition			
Blaine fineness, cm²/g	3390	4000	-
MgO, %	1.2	5.32	-
SO_3, %	2.23	-	-
*LOI, %	2.15	0.33	-
Total alkali, %	0.51	-	-
Chloride, %	0.019	0.006	-

*LOI: Loss on Ignition

Fig. 1. Location and situation during taking seawater (33°35'42.3"N 130°06'39.6"E)

Table 2. Chemical composition of natural seawater

Specific gravity	pH	Chemical composition (g/L)					
		Cl^-	SO_4^{2-}	Ca^{2+}	Mg^{2+}	K^+	Na^+
1.030	7.71	18.72	2.37	0.36	1.2	0.35	9.9

2.2 Mix proportions

The mix proportions used in the mortar specimens are summarized in **Table 3**. The W/B ratio of the specimens was varied at 0.40, 0.50, and 0.60. Three types of mixes were

prepared for each W/B ratio – OPC with tap water as the reference, OPC with seawater, and GGBFS with seawater.

Table 3. Mix proportions

W/B	Unit Weight (kg/m³)					Remarks	
	Water		Binder		Sand		
	Tapwater	Seawater	OPC	GGBFS			
0.40	232	-	581	-	1508	Plain Bar Series*	-
	-	232	581	-	1525		
	-	232	291	291	1514		
0.50	255	-	510	-	1508	Plain Bar Series*	Different Bar Series
	-	255	510	-	1525		
	-	255	255	255	1515		
0.60	272	-	454	-	1508	Plain Bar Series*	-
	-	272	454	-	1508		
	-	272	227	227	1499		

*Specimen which only plain steel bars were embedded

2.3 Specimen design

The specimen dimensions were set at 150 × 100 × 150 mm^3 with concrete cover of 50 mm was cas on each specimen as shown in **Fig. 2**. The specimens were demolded 24-hour after casting and cured (continued immersion) for 28 days. Later, five of the specimen surfaces (except measurement surface) were painted with epoxy resin before being subjected to alternate wetting-drying cycles. Each cycle included 7 days with 2 days of wetting (immersed in tap water or seawater) and 5 days of drying (air drying). It should

be noted that the curing water and exposure water (i.e., water in the wetting-drying cycles) was the same. The details of various specimens subjected to wetting-drying are presented in **Table 4**.

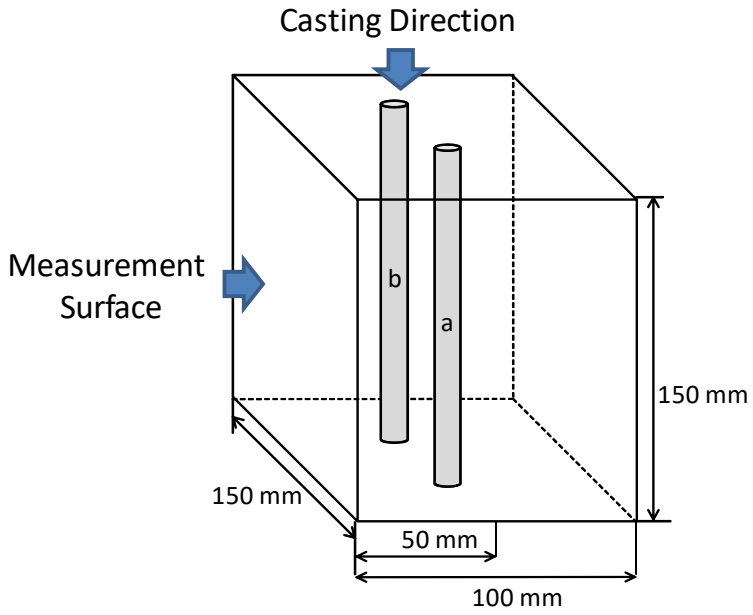

Fig. 2. Specimen dimensions and shape

Table 4. Details of cured specimens subjected to wetting-drying cycles

Case	Mix-Cure	Mixing	Curing$^{28\ days}$* + Wet-dry Cycles (2/5)$^{after\ 28\ days}$
I	T-T	Tap water	Tap water
II	S-T	Seawater	Tap water
III	T-S	Tap water	Seawater
IV	S-S	Seawater	Seawater

*Continued immersion for 28 days.

2.3.1 Plain bar series

Three different W/B ratios were used in the plain bar series, 0.40, 0.50, and 0.60. For each W/B ratio, six different specimens were prepared. Two plain reinforcing bars (ϕ-13) were embedded in each specimen (see **Fig. 2**). Later, the specimens were set up in to various cases according **Table 4**. The details of specimens type in the plain bar series are listed in **Table 5**.

Table 5. List of specimens – Plain bar series

W/B	Specimen	Unit Weight (kg/m³)					Case			
		Water		Binder		Sand	I	II	III	IV
		Tap	Sea	C	GG BFS		Mix: Curing			
							T-T	S-T	T-S	S-S
0.4	N40/T-T	232	-	581	-	1508	Δ			
	N40/T-S	232	-	581	-	1508			Δ	
	N40/S-T	-	232	581	-	1525		Δ		
	N40/S-S	-	232	581	-	1525				Δ
	B40/S-T	-	232	291	291	1514		Δ		
	B40/S-S	-	232	291	291	1514				Δ
0.5	N50/T-T	255	-	510	-	1508	Δ			
	N50/T-S	255	-	510	-	1508			Δ	
	N50/S-T	-	255	510	-	1525		Δ		
	N50/S-S	-	255	510	-	1525				Δ
	B50/S-T	-	255	255	255	1515		Δ		
	B50/S-S	-	255	255	255	1515				Δ
0.6	N60/T-T	272	-	454	-	1508	Δ			
	N60/T-S	272	-	454	-	1508			Δ	
	N60/S-T	-	272	454	-	1508		Δ		
	N60/S-S	-	272	454	-	1508				Δ
	B60/S-T	-	272	227	227	1499		Δ		
	B60/S-S	-	272	227	227	1499				Δ

Δ : specimen made

2.3.2 Different bar series

In different bar series, only a 0.50 W/B ratio was used. The dimensions of the specimens are as shown in **Fig. 2**. A summary of reinforcing bar types (PS, EC, and SS) is presented in **Table 6** and **Fig. 3**. Half of all the EC bars were damaged artificially in the middle (scratch), as shown in **Fig. 3**; these bars are noted as "EC-D" (damaged). Different specimens and their notations are listed in **Table 7**.

Table 6. Types of reinforcing bars

Reinforcing bar type	Diameter	Symbol
Epoxy-coated damaged (D)	D13	EC-D
Epoxy-coated no damage (ND)	D13	EC-ND
Stainless-steel SUS304-SD	D13	SS
Plain steel	ϕ-13	PS

Fig. 3. Setting up and types of reinforcing bars

Table 7. List of specimens in different bar series

Type	Specimen Name*	W/B	Case			
			Mixing-curing			
			I	II	III	IV
			T-T	S-T	T-S	S-S
N (OPC)	N-EC-D	50%	Δ	Δ	Δ	Δ
	N-EC-ND			Δ	Δ	Δ
	N-SS			Δ	Δ	Δ
	N-PS		Δ	Δ	Δ	Δ
B (GGBFS)	B-EC-D	50%		Δ		Δ
	B-EC-ND			Δ		Δ
	B-SS			Δ		Δ
	B-PS			Δ		Δ

*Example: N-EC-D/T-T(OPC–Epoxy Coated–Damage/Tap-water mix–Tap-water curing)

3. EXPERIMENTAL OUTLINE

3.1 Half-cell potential (HCP)

According to ASTM C876-09 [24], half-cell potential measurement is an electrochemical technique that determines corrosion behavior (**Table 8**). The corrosion potential, E_{corr} (half-cell rebar/concrete), is measured as a potential difference (volts) against a reference electrode (half-cell) [25]. A more negative voltage reading implies that the embedded bar has excess electrons and there is, therefore, a higher likelihood of the bar corroding [26]. In this study, time-dependent changes in corrosion were monitored by half-cell potential (E_{corr}) measurement at ~1 h from the end of the wet-cycle using a portable rebar corrosion meter type SRI-CM-II (see **Fig. 4**) then convert to Copper

Sulafate Electrode (CSE). For each condition, 2 to 4 bars were tested and the values were averaged.

Fig. 4. Half-cell potential measurement

Table 8. Corrosion probability (ASTM C876-09)

Half-cell potential (V, CSE)	Corrosion activity
–200 < E	90% no corrosion probability
–350 < E < -200	uncertainty
E < –350	90% corrosion probability

ASTM C876-09 has recommendation that the standard for judgment corrosion probably may not be suitable for epoxy-coated bar. In market, epoxy-coated bar consist of two type of bar regarding the electrical circuitry. One type completely hinder electrical circuitry, other type still allow the electrical circuitry. Therefore, preliminary investigation was conduct in order to check the suitability of the ASTM C876-09 for the epoxy-coated

bar particularly for different bar series in this study. The schematic of potential measurement is shown in **Fig. 5**. Four reinforcing bars were immersed in 3% aqueous NaCl. The different bars tested were plain bars (PS), epoxy-coated bar no damage (EC-ND), epoxy-coated bar damage-1 (EC-D1), and epoxy-coated bar damage-3 (EC-D3). Scratch areas were artificially created using a cutter knife in the middle part of the reinforcing bars. The results obtained indicate that the potentials of different bar types were similar, as shown in **Fig. 6**. This implies that epoxy painting did not hinder the electrical circuitry. Therefore, it is possible to measure half-cell potential using the ASTM C876-09 standard.

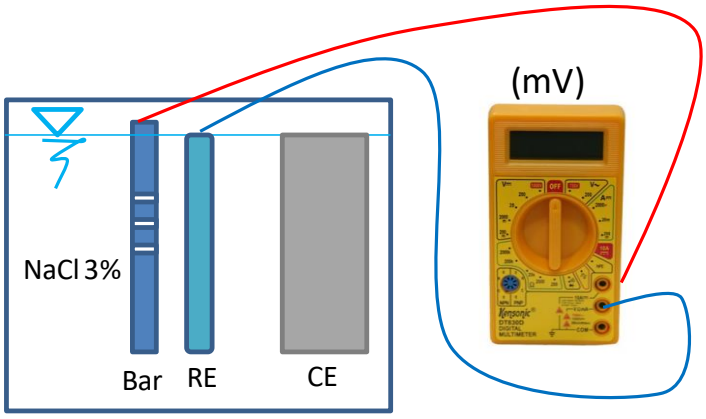

Fig. 5. Schematic of the electrical circuitry used for potential evaluation

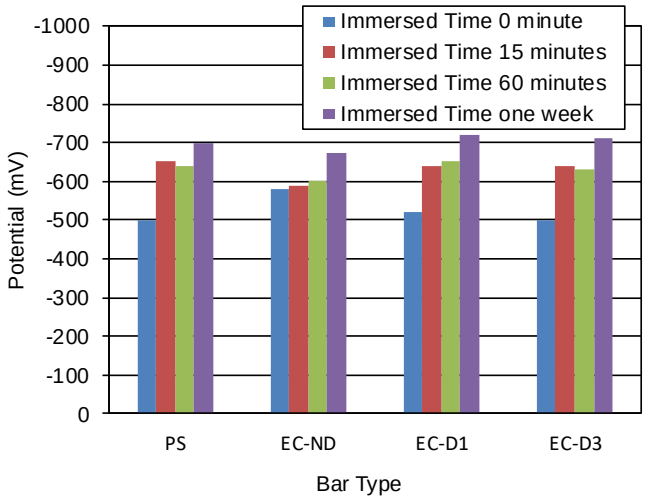

Fig. 6. Potential of each bar type

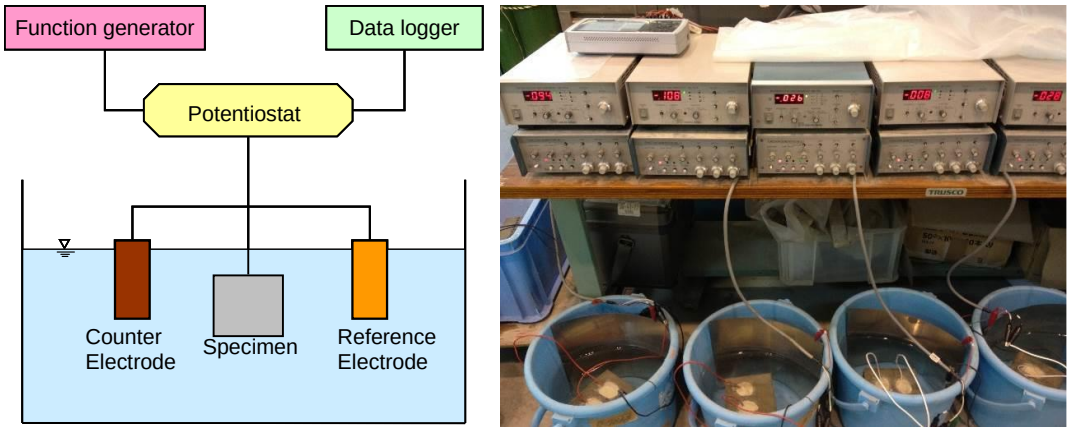

Fig. 7. Anodic-cathodic polarization curve measurement by immersion method

3.2 Anodic-cathodic polarization curves

The generation of polarization curves by the immersion method is described in **Fig. 7**. When anodic current increases, it means that the passivity of the film on steel bars

worsens, as presented in **Fig. 8a**. When the cathodic current becomes larger, it means that the supply of oxygen to the steel surface increases (**Fig. 8b**). Polarization-curve measurement takes about 40 min during which the specimen should be immersed in a water. During measurement, the potential of the steel bar (E_{corr}) shifted to ±700 mV from the natural potential at a sweep rate of 50 mV/min. The maximum current density obtained from the anodic polarization curves in **Fig. 8a** was then used to judge the grade of passivity. Further, standards for evaluating the grade of passivity in anodic polarization curves were sourced from the work published by Otsuki [27] (**Table 9**).

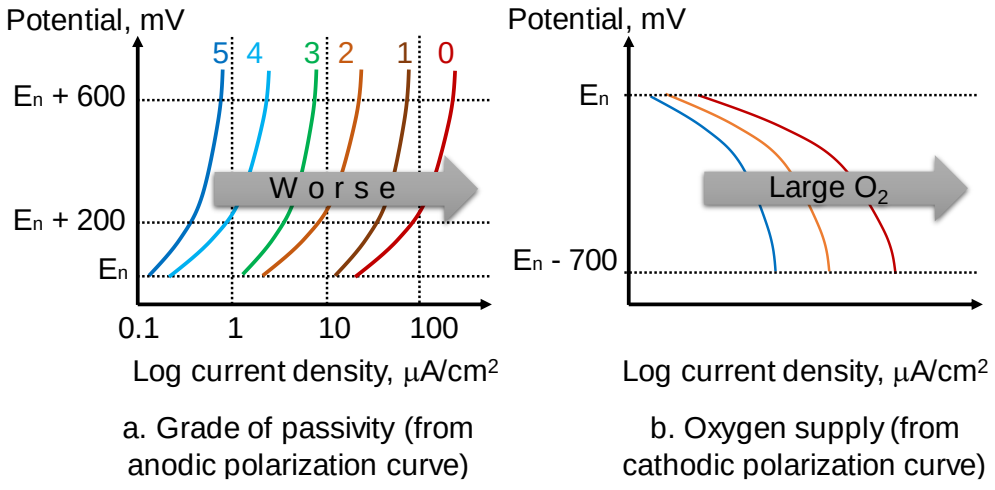

Fig. 8. Evaluation of anodic-cathodic polarization curves [27]

Table 9. Grade of film passivity associated with the polarization curves

Grade	Polarization curve	Condition
Grade 0	potential 0.2–0.6 V, current density is over 100 μA/cm² at least one time	no passivity
Grade 1	potential 0.2–0.6 V, current density is 10–100 μA/cm²	limited degree of passivity
Grade 2	potential 0.2–0.6 V, current density is higher than 10 μA/cm² at least once but does not qualify as Grade 1	
Grade 3	potential 0.2–0.6 V, current density is 1–10 μA/cm²	
Grade 4	potential 0.2–0.6 V, current density is over 1 μA/cm² at least once but does not qualify as Grade 1, 2 and 3.	
Grade 5	potential 0.2–0.6 V, current density is less than 1 μA/cm²	excellent passivity

3.3 Chloride ion distribution

Chloride ion concentration was measured at given specimen depths. For this test, cylindrical specimens were prepared by coring and then cut in three layers (each 10 mm thick) from the surface of concrete and crushed into powder. Chloride ion concentration in concrete layers was determined according to JSCE-G573-2003 [28].

4. RESULTS AND DISCUSSION

4.1 Half-cell potential (HCP)

4.1.1 Plain bar series

The HCPs of plain bar series at W/B ratios of 0.40, 0.50, and 0.60 in various scenarios are plotted in **Fig. 9**. Firstly, Case-I (T-T) for tap-water mixing and curing indicated a 90% probability of no corrosion at 100–200 mV. Case-I specimens at W/B = 0.50 approached and crossed the potential threshold for corrosion at the end of the test (4 years).

Here, it should be emphasized that tap water is suitable and recommended as mixing and curing water.

In the early stages, seawater mixing in Case-II (S-T) resulted in a higher negative potential (>–350 mV). However, after 6 months of exposure, the potential moved in a positive direction despite using seawater for mixing. This might be because chloride from the seawater was washed by tap water during curing and in the wetting-drying process. In addition, the microstructure of the mortar might have improved due to an acceleration in hydration in the presence of chloride ions from seawater [6]. Further, the potential of GGBFS specimens was more positive when compared to that of OPC specimens in Case-II (S-T). In the case of B40/S-T at 400 days, the potential dropped drastically and anomalously, but later recovered and approached that of N40/S-T. Therefore, the influence of curing conditions and cement type is more significant than that of seawater [29].

The potential at ~–600 mV during wetting-drying cycles was showed by tap-water mixing and seawater curing on Case-III (T-S). Accelerated corrosion due to wetting-drying ensures sufficient oxygen supply and diffusion of chloride ions. Moreover, the wetting-drying process influences the motion of Cl^-. During this process, the mortar absorbs a number of Cl^- ions after which the potential rapidly drops due to the abundance of chloride ions in seawater used for curing and wetting-drying. Thus, seawater, when used as curing water and in the wetting-drying process, greatly affects the potential.

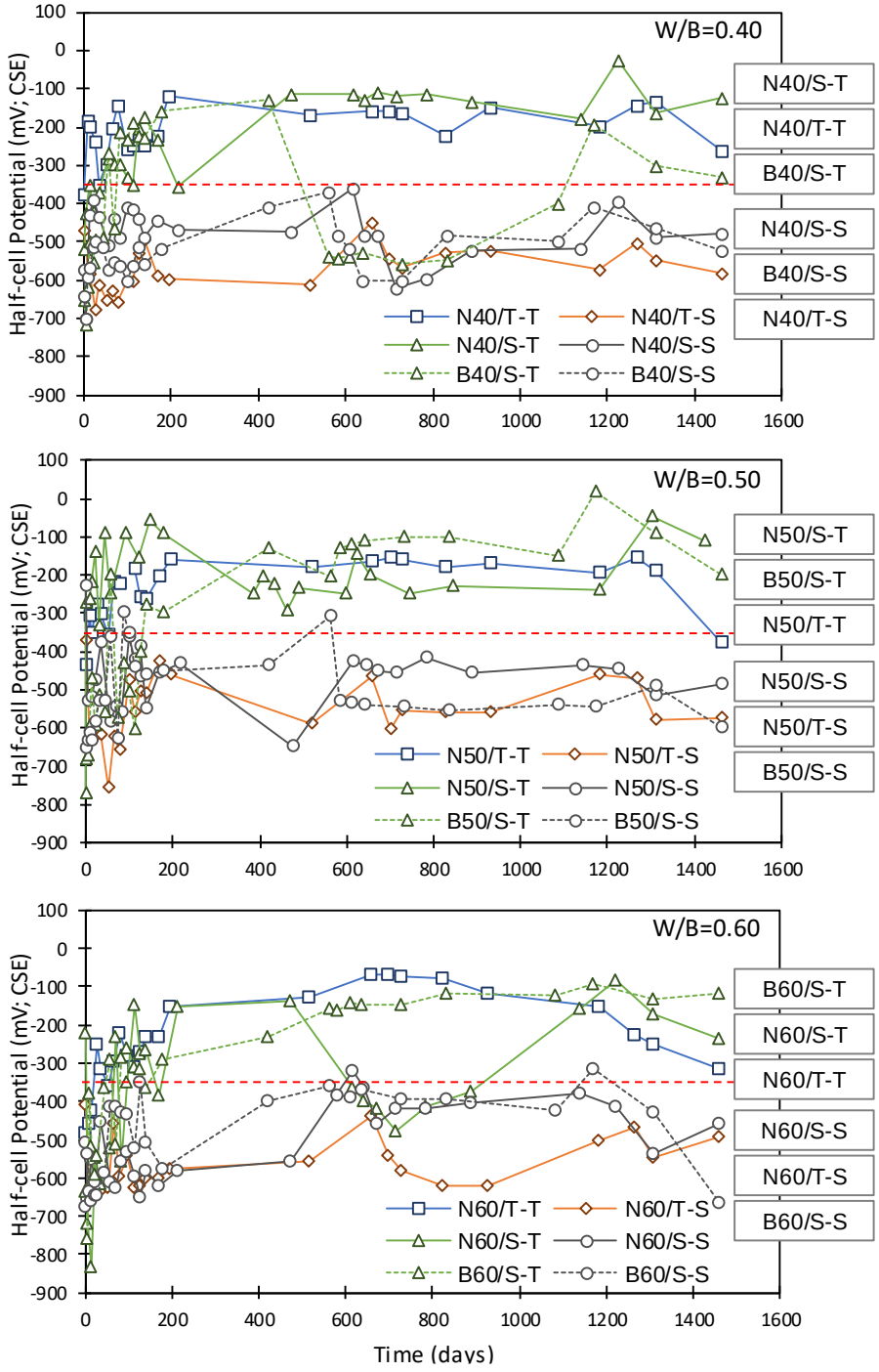

Fig. 9. Half-cell potential of the plain bar series

The specimen in Case-IV (S-S) with seawater for both mixing and curing has a potential of ~500 mV during wetting-drying, which indicates a 90% probability of corrosion. The potential at all W/B ratios remained similar. It is considered that the concentration of chloride ions in seawater used was the same in mixing and wetting-drying cycles. In other words, chloride ion concentration was saturated. These observations imply that the W/B ratio has little effect on the potential in Case-IV.

The half-cell potential of GGBFS showed tendencies similar to that of OPC, particularly in Case-IV (S-S), irrespective of the W/B ratio (**Fig. 9**). It is should be underlined that the half-cell potential of GGBFS particularly in the very early-age. The potentials of the steel bars were more negative than –800 mV. GGBFS is a glassy by-product of iron-making and contains manganese and other species such as sulfides (S^{2-}, HS^{-}, and Sn^{2-}) that induce a reducing effect and lead to an extremely high negative potential [30]. However, the potentials of GGBFS specimens tend to recover over a period of 200 days, particularly with tap-water curing. From the half-cell potential results, it can be noted that seawater used for curing leads to a lower potential (more negative potential) than seawater used for mixing mortar.

4.1.2 Different bar series

Two types of reinforcing bars (reference), plain steel bar (PS) and epoxy-coated bars with damage (EC-D) were subjected to tap-water mixing and curing in Case-I (T-T) (**Fig.**

10). The specimens in Case-I consisted of only OPC. Both PS and EC-D showed a higher positive potential (more than –250 mV) during wetting-drying cycles. Over a period of 1200 days, the potential of EC-D was slightly higher than that of PS. However, both types of bars exhibited a corrosion probability greater than 90% over a period of 1400 days in wetting-drying cycles. This result implies that if damage exists, over a period of time, even epoxy-coated bars become vulnerable to corrosion.

There are four types of reinforcing bars embedded in specimens made with OPC and GGBFS (Case-II (S-T)), as shown in **Fig. 10**. The reinforcing bars include EC-D, EC-ND, SS, and PS bars. The half-cell potential of OPC and GGBFS specimens were similar during exposure. Both these specimens with different types of bars with seawater as mixing water showed potentials higher than –200 mV (90% probability of no corrosion). This implies that the effect of curing water is more significant than that of mixing water. In addition, in most cases, GGBFS was superior to OPC in Case II (S-T).

The HCPs of specimens with four types of bars embedded with tap-water mixing and seawater curing in Case-III (T-S) are shown in **Fig. 10**. In Case-III for different bar series, the specimens were made with OPC alone. This case mimics marine conditions, especially the tidal and splash zones, where concrete is directly exposed to seawater. Only the potential of N-PS/T-S crossed the corrosion threshold of –350 mV in a period of 200 days. Other types of bars crossed the threshold value after 1305 days. The corrosion resistance for different bar types follows the order of EC-ND > SS > EC-D > PS.

Therefore, in high chloride environments, corrosion-resistant reinforcing bars are needed, such as epoxy-coated bars or stainless steel bars, which have a high chloride threshold value (CTV).

The HCPs of specimens with seawater mixing and curing in Case-IV (S-S) are shown in **Fig. 10**. Four types of bars were embedded in Case-IV specimens made with OPC and GGBFS. After 175 days of wetting-drying, only the PS bars in OPC showed a potential more negative than –400 mV and it remained stable during wetting-drying cycles. Therefore, when seawater was used both as mixing and curing water, the risk of corrosion in reinforcing bars increased.

The potential of GGBFS specimens was more positive than that of OPC specimens in Case-IV (S-S) for all types of bars except EC-D (**Fig. 10**). Further, EC-D, EC-ND, and SS bars showed a potential more positive than –300 mV. These observations indicate that PS bars had the least corrosion resistance. This considered that in the case of high corrosion resistance bar such us epoxy-coated and stainless steel bar were used, then seawater more applicable to use as mixing and curing agent. Further, it is suggested that steel bar with lower corrosion resistance, then GGBFS (i.e., SCMs) was recommended when using seawater as mixing and curing agent. The half-cell potential of different bar series is strongly correlated with the half-cell potential of plain bar series. It can be reported that seawater used for curing water influences corrosion potential to a greater extent than that used for mixing.

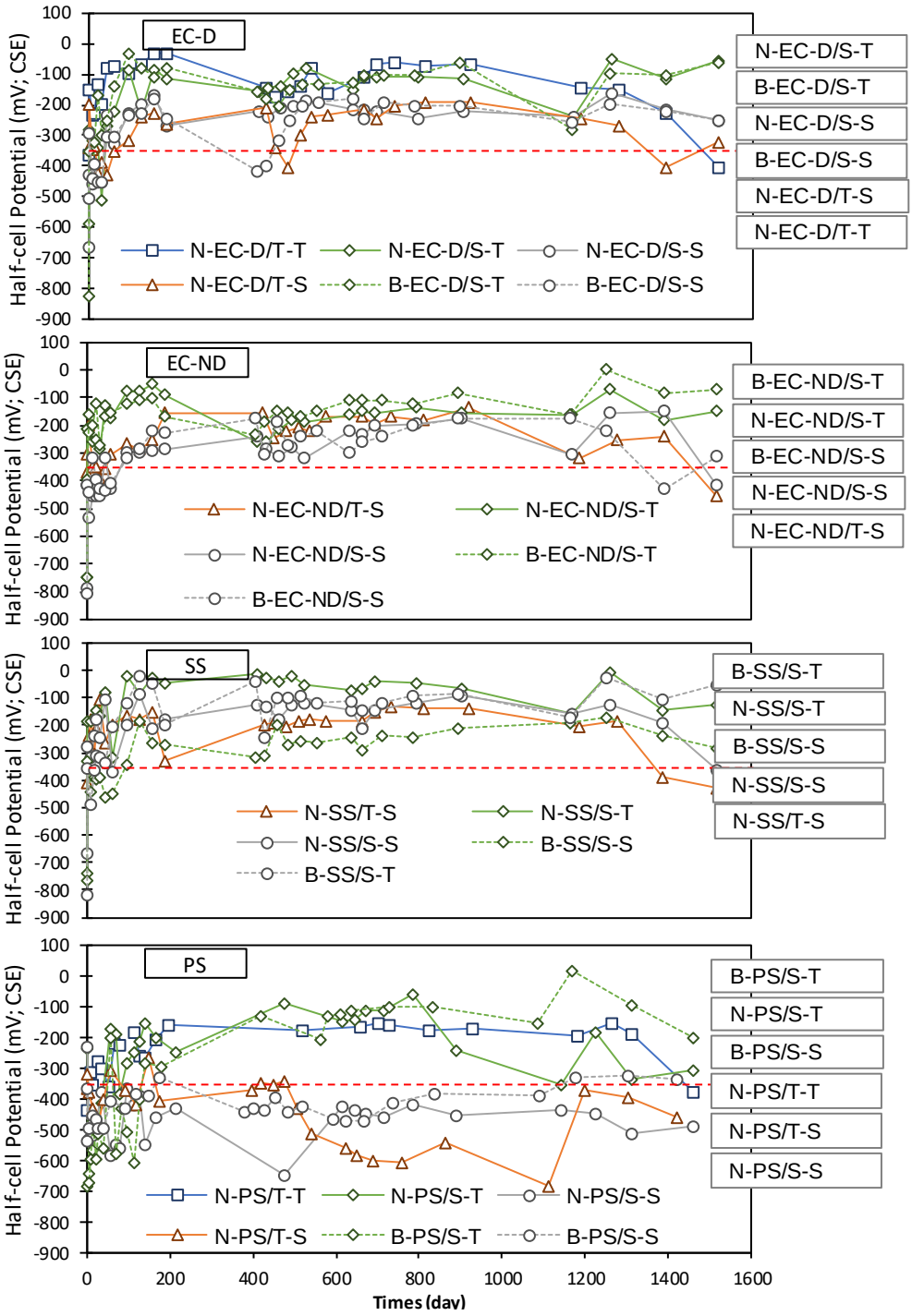

Fig. 10. Half-cell potential of different bar series

4.2 Anodic-cathodic polarization curves

4.2.1 Plain bar series

The maximum anodic current values calculated from the polarization curves for different cases are shown **Fig. 11**. **Table 10** presents a summary of the maximum anodic and cathodic current with passivity grades for different specimens. In the early stages (0 months), the specimens in Case-I (T-T) were categorized as Grade 3 with a maximum anodic current of 5 μA/cm². At 6 months, the maximum anodic current reduced. The maximum anodic current of specimen followed the order N60T-T < N50T-T < N40T-T. After 36 months of exposure, the order of N40T-T < N50T-T < N60T-T was observed. This indicates that anodic current reduced with an increase in specimen age or in other words, after cement hydration. Further, it is seen that anodic current is significantly affected by the W/B ratio (anodic current reduces when the W/B ratio decreases).

The maximum anodic currents derived from the anodic polarization curves for specimens OPC and GGBFS with seawater mixing and tap-water curing (Case-II (S-T)) are presented in **Fig. 11**; the corresponding passivity grades are summarized in **Table 10**. The maximum anodic current of steel bars with OPC tends to be higher than that of GGBFS after 24 months. Furthermore, in the cathodic polarization curve, the maximum cathodic current of OPC was higher than that of GGBFS after 18 months. This phenomenon can be attributed to the low pore volume of the cement matrix in GGBFS mortar and the reduction action of GGBFS powder. It should be noted that GGBFS

powder was produced in a reductive atmosphere and the oxidation number of Fe or Mn in GGBFS is low [31]. This means that the amount of oxygen around the steel bar in GGBFS decreased. Thus, from the perspective of cathodic polarization curves, GGBFS is effective in reducing the risk of corrosion posed by seawater used in the mixing process [8].

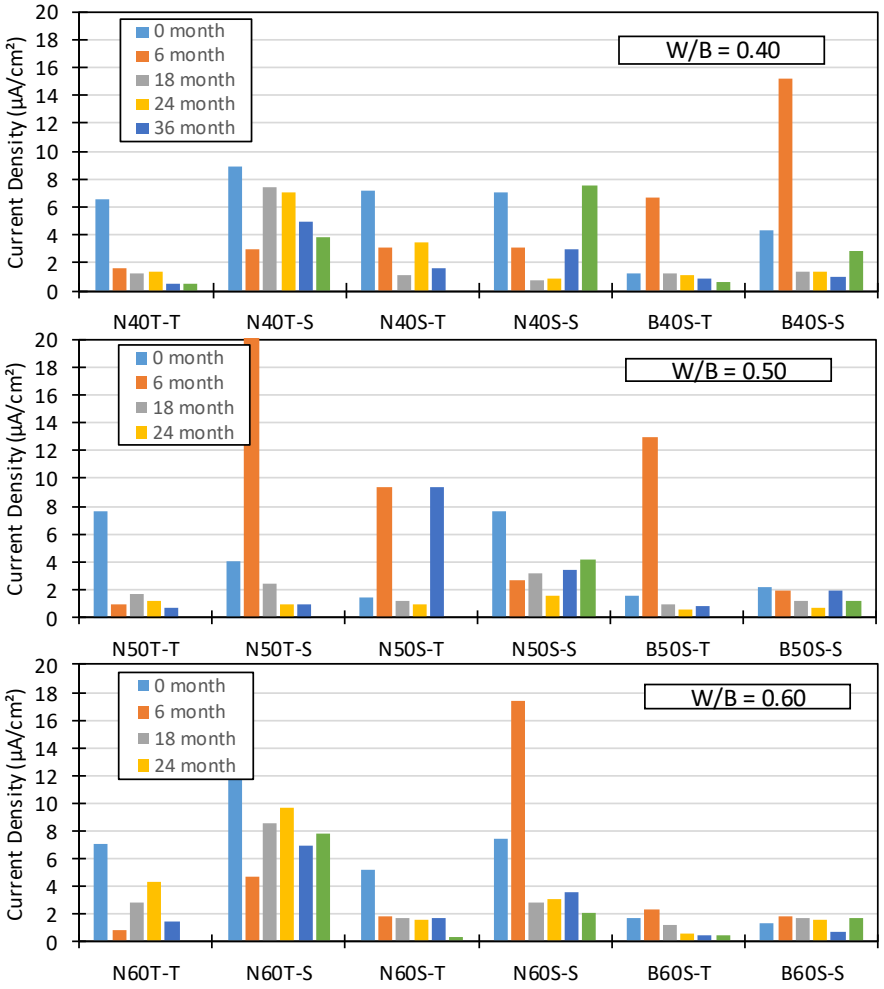

Fig. 11. Maximum anodic current derived from the anodic polarization curves of plain bar series

Table 10. Maximum anodic/cathodic current and passivity grade (plain bar series)

W/C	Specimen	Maximum Anodic/Cathodic Current, μA/cm²/ Passive Grade					
		Passive Grade					
		0 month	6 month	18 month	24 month	36 month	48 month
40	N40/T-T	6.51/28.61	1.66/4.07	1.21/3.31	1.32/1.66	0.52/2.65	0.53/2.61
		3	4	4	4	5	5
	N40/T-S	8.90/30.45	3.03/9.38	7.48/8.91	7.00/8.01	4.91/5.69	3.89/0.86
		3	4	3	3	4	4
	N40/S-T	7.23/18.59	3.11/18.72	1.13/3.35	3.43/7.00	1.60/4.86	-/-
		3	4	4	4	4	
	N40/S-S	7.04/28/88	3.15/35.32	0.80/4.42	0.90/2.29	2.95/2/69	7.52/8/28
		3	4	5	5	4	3
	B40/S-T	1.28/2.24	6.73/24.85	1.24/2.19	1.08/1.31	0.93/4.22	0.69/1.54
		4	3	4	4	5	5
	B40/S-S	4.31/28.88	15.18/31.98	1.35/1.81	1.37/1.01	1.05/2.54	2.84/2.10
		4	2	4	4	4	4
50	N50/T-T	7.69/12.45	0.98/4.18	1.68/2.99	1.21/2.82	0.77/7.65	-/-
		3	5	4	4	5	-
	N50/T-S	4.02/1.47	30.89/35.53	2.40/2.84	0.90/3.10	0.91/0.90	-/-
		4	2	4	5	5	-
	N50/S-T	1.43/15.84	9.37/2.34	1.21/3.89	0.90/4.03	9.37/3.15	-/-
		4	3	4	5	3	-
	N50/S-S	7.60/55/46	2.63/8.93	3.22/7.22	1.52/4.33	3.40/4.73	4.15/6.66
		3	4	4	4	4	4
	B50/S-T	1.55/3.88	12.97/4.03	1.01/3.31	0.62/1.40	0.81/1/76	-/-
		4	2	4	5	5	-
	B50/S-S	2.21/1.18	1.91/1.80	1.16/2.19	0.73/1.14	1.91/1.80	1.19/0.20
		4	4	4	5	4	4
60	N60T-T	7.07/13.18	0.83/4.62	2.76/3.23	4.28/2.28	1.42/8.61	-/-
		3	5	4	4	4	-
	N60/T-S	12.02/26.87	4.70/10.16	8.49/15.15	9.61/7.84	6.95/8.24	7.77/11.92
		2	4	3	3	3	3
	N60/S-T	5.12/42/04	1.81/4/82	1.67/6.07	1.53/2.95	1.67/1.80	0.28/0.55
		3	4	4	4	4	5
	N60/S-S	7.38/43.63	17.32/70.77	2.84/8.18	3.04/4/13	3.58/5.56	2.07/5/70
		3	2	4	4	4	4
	B60/S-T	1.61/4.00	2.32/5.48	1.14/2.95	0.60/1.34	0.42/0.89	0.38/2.73
		4	4	4	5	5	5
	B60/S-S	1.34/43.63	1.81/4.82	1.67/4.93	1.52/2.82	0.64/2.10	1.67/2.25
		4	4	4	4	5	4

Fig. 11 shows the anodic polarization curve of OPC with tap-water mixing and seawater curing for Case-III (T-S). In the very early stages (less than one month), all the specimens were categorized at Grade 3 (see **Table 10**) with a maximum anodic current of

~10 μA/cm². However, after 6 months of wetting-drying cycles, the maximum anodic current reduced to less than 5 μA/cm² with passivity at Grade 4. If compared to Case-I (T-T), seawater, when used as curing water, clearly increased the maximum current in the anodic polarization curve. Seawater, when used as curing water, tends to cause dampness that provides good electrolytic action between the anodic and cathodic regions of the embedded steel bar, thereby accelerating the corrosion process [9].

The polarization curves of specimens OPC and SCM with GGBFS50% with seawater mixing and curing in Case-IV (S-S) are presented in **Fig. 11** and their passivity grades are listed in **Table 10**. In the very early stages (0 months), the GGBFS specimen exhibits lower maximum anodic current than the OPC specimen. After 6 months, the anodic result followed an opposite pattern and OPC exhibited a lower value than GGBFS, except for specimen N60S-S. However, after 36 months and 48 months of interaction with seawater and wetting-drying cycles, GGBFS showed better passivity than OPC specimens [22, 32]. This is probably because SCMs take a long time to complete cement hydration. Furthermore, their higher resistivity to corrosion probably increased due to the properties of GGBFS concrete, such as Cl^- immobilization, low porosity, and the low content of oxygen [8].

4.2.2 Different bar series

The maximum currents derived from anodic/cathodic polarization curves and

passivity grades for different specimens are summarized in **Table 11**. **Fig. 12** shows the maximum anodic currents of OPC specimens with tap-water mixing and curing in Case-I (T-T). Only two types of steel bars were used in this case – plain bars (N-PS/T-T) and epoxy-coated bars with small artificial uncoated (scratch) areas (N-EC-D/T-T). When exposed to wetting-drying cycles, N-EC-D/T-T bars showed good passivity and generated a very small anodic current when compared to N-PS/T-T. This implies that epoxy-coated bars showed good passivity and the coating protected steel bars from corrosion.

The maximum currents calculated from the anodic polarization curves of specimens made with OPC and GGBFS mixed with seawater and cured with tap water in Case-II (S-T) are shown in **Fig. 12**. Four types of bars, viz. PS, EC-D, EC-ND, and SS, were used. In all bar types, specimens with GGBFS showed better passivity than OPC specimens after 18 months. Further, the lowest corrosion resistance due to seawater mixing was exhibited by plain bars.

Fig. 12 shows the maximum current derived from the anodic polarization curves of OPC specimens with tap-water mixing and seawater curing (Case-III (T-S)). Four types of bars were used – PS, EC-D, EC-ND, and SS. The maximum anodic current of SS bars stabilized during exposure and it was higher than that of PS bars. It may be theorized that the stainless steel used, SUS304-SD, with a high chloride threshold value of 15 kg/m^3, experiences a smooth flow of electricity due to the presence of chloride in seawater used for curing, which assists in anodic reactions.

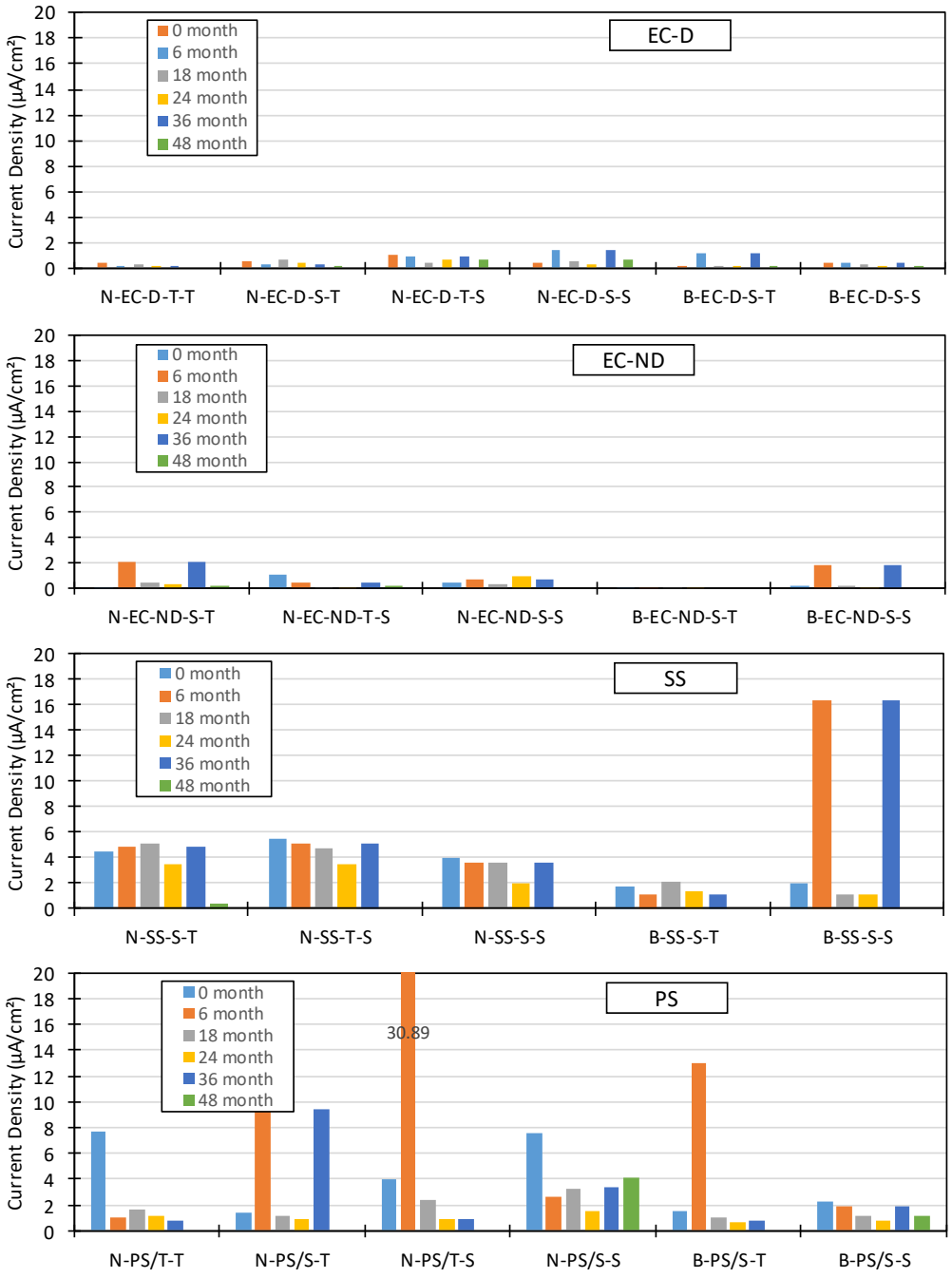

Fig. 12. Maximum anodic current derived from the anodic polarization curves of different bar series

Table 11. Maximum anodic/cathodic current and passivity grade (different bar series)

Case	Specimen	Maximum Anodic/Cathodic Current, μA/cm²					
		Passivity Grade					
		0 month	6 month	18 month	24 month	36 month	48 month
I	N-EC-D/T-T	0.37/0.57	0.09/0.27	0.33/0.04	0.13/0.57	0.09/0.27	-
		5	5	5	5	5	-
I	N-PS/T-T	7.69/12.45	0.98/4.18	1.68/2.99	1.21/2.82	0.77/7.65	-/-
		3	5	4	4	5	-
II	N-EC-D/S-T	0.53/1.00	0.33/2.24	0.62/1.11	0.39/0.95	0.33/2.24	0.21/1.30
		5	5	5	5	5	5
II	N-EC-ND/S-T	0.05/0.06	2.12/36.00	0.39/0.31	0.38/0.23	2.12/36.00	0.18/-
		5	4	5	5	4	5
II	N-SS/S-T	4.43/2.84	4.81/6.42	5.06/2.33	3.51/1.35	4.81/6.42	0.39/3.01
		4	4	3	4	4	5
II	N-PS/S-T	1.43/15.84	9.37/2.34	1.21/3/89	0.90/4.03	9.37/3.15	-/-
		4	3	4	5	3	-
II	B-EC-D/S-T	0.17/0.45	1.16/2.36	0.10/0.52	0.08/0.24	1.16/2.36	0.08/0.35
		5	4	5	5	4	4
II	B-EC-ND/S-T	0.03/0.06	0.01/0.04	0.05/0.07	0.03/0.05	-/0.15	-
		5	5	5	5	-	-
II	B-SS/S-T	1.71/0.61	1.13/1.14	2.07/1.37	1.35/0.70	1.13/1.14	-/-
		4	4	4	4	4	-
II	B-PS/S-T	1.55/3.88	12.97/4.03	1.01/3/31	0.62/1.40	0.81/1.76	-/-
		4	2	4	5	5	-
III	N-EC-D/T-S	1.06/0.89	0.91/3.80	0.44/1.03	0.64/1.37	0.92/1.77	0.71/3.41
		4	5	5	5	5	5
III	N-EC-ND/T-S	1.11/0.64	0.39/0.52	0.13/0.18	0.11/0.10	0.39/0.52	0.25/0.91
		4	5	5	5	5	5
III	N-SS/T-S	5.48/2.29	5.10/2.69	4.75/1.93	3.51/1.35	5.10/2.69	-/-
		3	3	4	4	3	-
III	N-PS/T-S	4.02/1.47	30.89/35.53	2.40/2.84	0.90/3.10	0.91/0.90	-/-
		4	2	4	5	5	-
IV	N-EC-D/S-S	0.44/0.66	1.42/0.91	0.56/2.01	0.36/1.44	1.42/0.91	0.63/0.56
		5	4	5	5	4	5
IV	N-EC-ND/S-S	0.40/0.26	0.73/0.87	0.36/0.36	0.95/0.49	0.73/0.87	-/-
		5	5	5	5	5	-
IV	N-SS/S-S	3.98/2.84	3.59/3/32	3.56/2.19	2.01/0.77	3.59/3.32	-/-
		4	4	4	4	4	-
IV	N-PS/S-S	7.60/55.46	2.63/8.93	3.22/7.22	1.52/4.33	3.40/4.73	4.15/6.66
		3	4	4	4	4	4
IV	B-EC-D/S-S	0.47/0.34	0.42/0.58	0.28/0.52	0.15/0.28	0.42/0.58	0.20/0.73
		5	5	5	5	5	5
IV	B-EC-ND/S-S	0.14/0.07	1.84/1.49	0.18/0.15	0.13/0.08	1.84/1.49	-/-
		5	4	5	5	4	-
IV	B-SS/S-S	2.04/0.60	16.36/4.47	1.16/2.19	1.14/0.51	16.36/4.47	-/-
		4.0	2.0	4.0	4.0	2.0	-
IV	B-PS/S-S	2.21/1.18	1.91/1.80	1.16/2.19	0.73/1.14	1.91/1.80	1.19/0.20
		4	4	4	5	4	4

The maximum anodic/cathodic current and passivity grades of OPC and GGBFS specimens in Case-IV (S-S) are also reported in **Table 11**. The effectiveness of GGBFS in providing good passivity was especially prominent in the case of plain steel bars. In most cases with PS as the reinforcement, the maximum anodic current of specimens made with GGBFS were smaller than those of OPC specimens. It is suggested that the dense pore structure of GGBFS cement delayed the anodic reactions. Therefore, it can be proposed that GGBFS improves corrosion resistance in concrete mixed with seawater; this effect may be attributed to the low oxygen content in the cement matrix as well as Cl^- immobilization [8].

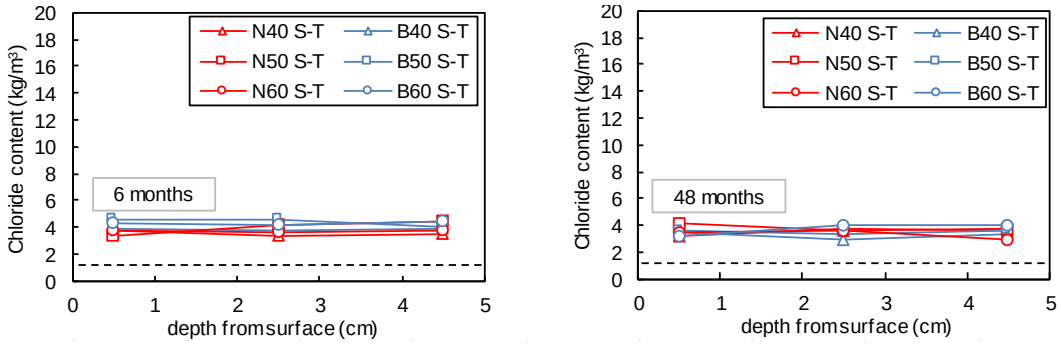

Fig. 13. Chloride distribution in Case-II (S-T)

4.3 Chloride distribution

Chloride ion distribution at 6 months and 48 months at various depths in Case-II (S-T) is shown in **Fig. 13**. The specimens were made with OPC and GGBFS with seawater

as mixing water and tap water as curing water. Chloride ion content at the surface is lesser than that in the interior of the bar. This implies that the abundance of chloride due to seawater mixing probably underwent washing in the OPC specimen in which tap water was used for curing and in the wetting-drying cycles. In contrary with GGBFS when using seawater as mixing water, undergone washing process were not happen so much compared with OPC even tap-water was used as curing water and in the wetting-drying cycles. This observation may be attributed to the dense pore structure of and Cl^- immobilization in GGBFS. Therefore, it may be stated that the W/B ratio has little effect on chloride penetration. In addition, chloride ion concentrations at different W/B ratios of 0.40, 0.50, and 0.60 are similar.

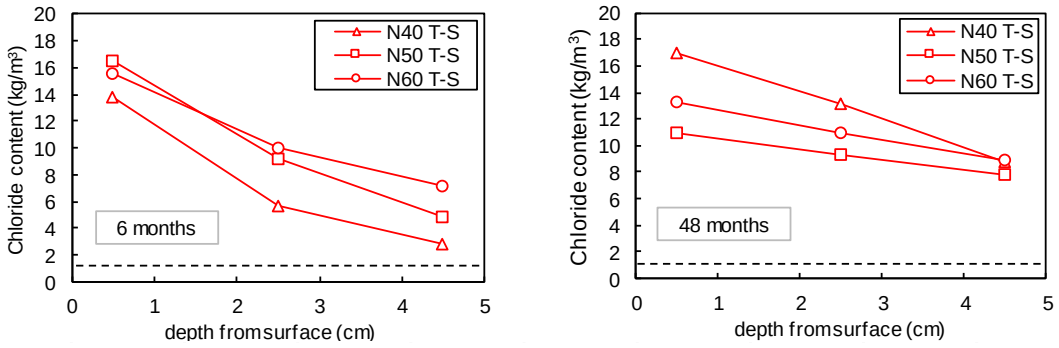

Fig. 14. Chloride distribution in Case-III (T-S)

The chloride ion distribution at 6 months and 48 months at various depths in Case-III (T-S) is shown in **Fig. 14**. The specimens in Case-III were made only with OPC

with tap-water mixing and seawater curing. Case-III mimics the real condition in marine environments, particularly in the tidal/splash zone. If a chloride content of 1.2 kg/m³ [33] is the threshold value for corrosion initiation, from **Fig. 14**, it can be seen that using reinforcement without protection, such as PS bars, leads to earlier corrosion. Further, the chloride ion concentration around the steel bar was similar at all W/B ratios after 48 months. This result implies that after long-term interaction with seawater, the effect of W/B ratio becomes negligible.

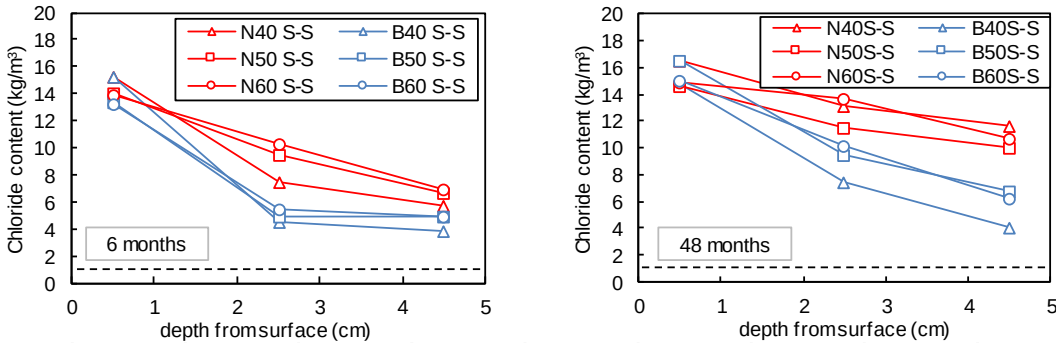

Fig. 15. Chloride distribution in Case-IV (S-S)

The chloride ion distribution in specimens made with OPC and GGBFS and mixed with seawater and cured for 6 months and 48 months (Case-IV (S-S)) is presented in **Fig. 15**. GGBFS exerts more resistance to chloride ion ingress [22, 32]. The specimen with GGBFS yielded a lower chloride content than OPC at both 6 months and 48 months. At 48 months, chloride content at the steel bar surface (40–50 mm depth) in GGBFS

specimens was 4.10 kg/m³ (B40/S-S), 6.70 kg/m³ (B50/S-S), and 6.20 kg/m³ (B60/S-S); these values were lower than those of OPC specimens –11.63 kg.m³ (N40/S-S), 9.97 kg/m³ (N50/S-S), and 10.62 kg/m³ (N60/S-S). This indicates that OPC specimens reinforced with steel bars are vulnerable to corrosion when seawater is used for mixing according to JSCE standards, which indicate that a chloride concentration of 1.2 kg/m^3 is necessary to initiate corrosion [28]. Further, both OPC and GGBFS specimens showed an increase in chloride ion concentration around the steel bar surface after 48 months. However, the increase was much lower in GGBFS specimens as compared to OPC. It is thought that GGBFS is responsible for the low porosity of the cement matrix as well as Cl^- immobilization [8].

4.4 Actual corrosion

After accelerated corrosion for 4 years in the wetting-drying process, the specimens were split up to evaluate the actual corrosion. The actual corrosion in PS bar series is presented in **Table 12**. During exposure, Case-I (as control) specimens, N40T-T, N50T-T, and N60T-T showed no corrosion. Case-II specimens showed some corrosion; however, both OPC and GGBFS showed only very small areas of corrosion on the steel bar surface. Probably tap water as curing water contain more oxygen oxygen than seawater as curing water. Wetting-drying cycles contribute to the motion of chloride ions or moisture into concrete. Once the oxygen level inside concrete is high enough, corrosion occurs in the

concrete. Therefore, dot corrosion is very possible on steel bar surfaces in Case-II. In addition, the initial chloride content in seawater (mixing water) can induce corrosion in the very early stages. However, after a period of time, corrosion resistance increases. Furthermore, steel bars must corrode to produce a passive film. This process begins soon after construction as cement hydration increases the pH of concrete. Because the use of seawater as mixing water extends the period of hydration, very little dot corrosion could be observed.

Table 12. Corrosion conditions (plain bar series)

W/C	Specimen Name	Curing Type			
		I	II	III	IV
		Mix : Curing			
		T : T	S : T	T : S	S : S
0.4	N40T-T	x			
	N40T-S			x	
	N40S-T		+		
	N40S-S				x
	B40S-T		+		
	B40S-S				x
0.5	N50T-T	x			
	N50T-S			x	
	N50S-T		+		
	N50S-S				+
	B50S-T		+		
	B50S-S				x
0.6	N60T-T	x			
	N60T-S			x	
	N60S-T		+		
	N60S-S				●
	B60S-T		+		
	B60S-S				+

Notation: x = no corrosion; + = dot corrosion; ● = area corrosion

Case-III specimens showed no corrosion on the bar surface. Although the chloride ion content crossed the threshold value, corrosion did not occur. In Case-IV in which seawater was used for mixing and curing, corrosion occurred. Dasar [34, 35] reported that after long-term exposure in marine tidal/splash zones, reinforced concrete (cover 30 mm; W/B ratio of 0.68) and prestressed concrete (cover 30 mm; W/B ratio of 0.47) without cracking were highly corroded. Thus, it was deemed that specimens with a 50 mm concrete cover vulnerable to corrosion if W/B ratio was larger than 0.30. Further, with an increase in the W/B ratio, the degree of corrosion in Case-IV followed the order of N60S-S > N50S-S > N40S-S. In addition, GGBFS exhibited good corrosion protection than OPC as observed in the actual corrosion data in Case-IV at all W/B ratios (**Table 12**).

In GGBFS specimens, corrosion occurred only in B60S-S. The actual corrosion conditions of N60S-S and B60S-S are shown in **Fig. 16**. At a low W/B ratio (0.27) [36] or with SCMs such as GGBFS [32, 37], steel corrosion in concrete mixed with seawater can be avoided even in existing reinforced concrete structures. Accordingly, if proper concrete design is conducted, seawater in concrete production may become acceptable. For the record, several bars corroded in the top of connection with wire portion (see **Fig. 16**). Corrosion in the connection portion might be attributed to the small gap between cable wire and the imperfectly coated connection portion. Thus, this part (~20 mm from the edge) should be excluded when evaluating the extent of corrosion.

Fig. 16. Actual corrosion of OPC and GGBFS specimens at a W/B ratio of 0.6 (Type IV)

The actual corrosion in different bar series is summarized in **Table 13**. It should be noted that only a W/B ratio of 0.50 was used in these series. According to the Standard Specifications for Concrete Structures (JSCE), the critical chloride ion concentration in carbon steel bars is 1.2 kg/m^3 [2]. Chloride ion content in seawater-mixed concrete was calculated to be 4.37 kg/m^3 at a W/B ratio of 0.50, which indicated that PS bars were highly vulnerable to corrosion. In epoxy-coated bars, corrosion occurred when chloride ion concentration at the steel bar surface was higher than 1.2 kg/m^3 [38]. However, if there were scratches on the coating, corrosion proceeded from that point. The critical chloride ion concentrations of SS bars (C_{lim}) are different depending on the grade of stainless steel used [39]. According to JIS G 4322, the chloride ion concentration SUS304-SD is 15

kg/m^3. The actual corrosion conditions for OPC specimens with seawater mixing and curing for four types of bars are shown in **Fig. 17**.

Table 13. Corrosion conditions (different bar series)

Type	Specimen Name	Curing Type			
		I	II	III	IV
		Mix : Curing			
		T : T	S : T	T : S	S : S
N	N-EC-D	x		x	
	N-EC-ND			x	
	N-SS			x	
	N-PS	x		x	
N	N-EC-D		x		x
	N-EC-ND		x		x
	N-SS		x		x
	N-PS		+		+
B	B-EC-D		x		x
	B-EC-ND		x		x
	B-SS		x		x
	B-PS		+		x

Notation: x = no corrosion; + = dot corrosion; ● = area corrosion

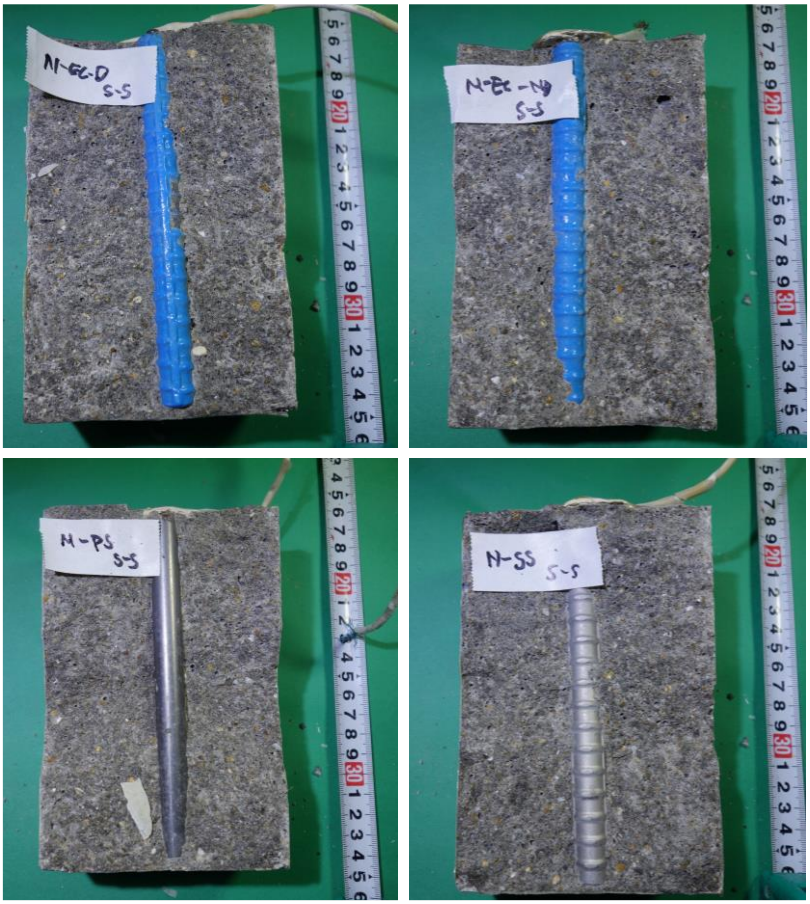

Fig. 17. Actual corrosion of OPC with a W/B ratio of 0.5 (Case-IV)

4.5 Corrosion activity of seawater as mixing and curing water

The degree of corrosion in steel bars after 4 years of interaction with seawater will be analyzed in this section to evaluate the applicability of seawater in concrete production. We shall particularly focus on the plain bar series, which has been demonstrated to exhibit the lowest corrosion resistance among all the types of steel tested. Qualitative measurements for the degree of corrosion are presented in **Table 15**, which was

constructed based on the criteria presented in **Table 14**. The relationship between degree of corrosion and time to initiate corrosion in each case is plotted in **Fig. 18**. The scale of degree of corrosion (total evaluation) ranges from 0 to 8.

Table 14. Criteria for evaluating the degree of corrosion

Evaluation item	Degree of corrosion		
	0	1	2
HCP	more positive than –200 mV	range –200 to –350 mV	more negative than –350 mV
Polarization curve	excellent passivity, anodic current less than 1 $\mu A/cm^2$	uncertain passivity, anodic current 1–100 $\mu A/cm^2$	no passivity, anodic current over 100 $\mu A/cm^2$
Chloride content at steel bar surface	negligible	below chloride threshold 1.2 kg/m^3	over chloride threshold 1.2 kg/m^3
Actual corrosion	negligible	dot corrosion	area corrosion

Table 15. Degree of corrosion at the end of the test

Evaluation type	Degree of corrosion					
	Case-I	Case-II		Case-III	Case-IV	
	OPC	OPC	GGBFS	OPC	OPC	GGBFS
Half-cell potential	2	0	0	2	2	2
Anodic polarization curve	0	1	0	1	1	1
Chloride content	0	2	2	2	2	2
Actual corrosion	0	1	1	0	2	1
Total evaluation	2	4	3	5	7	6

Evaluation items based on HCP value were adopted from ASTM C-816. Case-I (T-T) with tap water mixing and curing is referred to as the control specimen. The potential value of N50/T-T indicates a 90% probability of corrosion after 1400 days. Therefore, the

HCP value of PS bars in Case-I (T-T) set the threshold for corrosion initiation with respect to the degree of corrosion. HCP value was set us threshold time because the observation with the time-dependent changes recorded more intens rather than of polarization curve, chloride distribution and actual corrosion. This is a reasonable because the effect of seawater can be observed periodically. In addition, the degree of corrosion in Case-I according to the polarization curve, chloride distribution, and actual corrosion was negligible.

Case-II (S-T) showed a more positive potential (>–200 mV) at all W/B ratios during exposure until the end of the test. Here, it can be noticed that seawater, when used for mixing, did not have much influence on corrosion activity. Further, the HCPs of OPC and GGBFS specimens were similar. In contrast, the polarization curves of these specimens were very different. GGBFS exhibited superior passivity as compared to OPC. After 4 years of interaction with seawater, the maximum anodic current of GGBFS was smaller than that of OPC. Both OPC and GGBFS had a chloride content greater than the chloride threshold of 1.2 kg/m^3. The chloride content from seawater used for mixing contributed to the high chloride ion content in these specimens. In addition, very little dot corrosion occurred in both OPC and GGBFS.

In Case-III (T-S), which mimics marine tidal/splash zones, the HCP value tends to more negative (–600 mV). This corresponds with the anodic polarization curves, in which the maximum anodic current was greater than 1 μA/cm^2. Further, accelerated corrosion

due to wetting-drying ensures continuous movement of moisture or ions through the pores of the concrete matrix [40]. Therefore, chloride content around the steel bar was much higher than the threshold value of 1.2 kg/m^3. However, no corrosion was found on the steel bar surface.

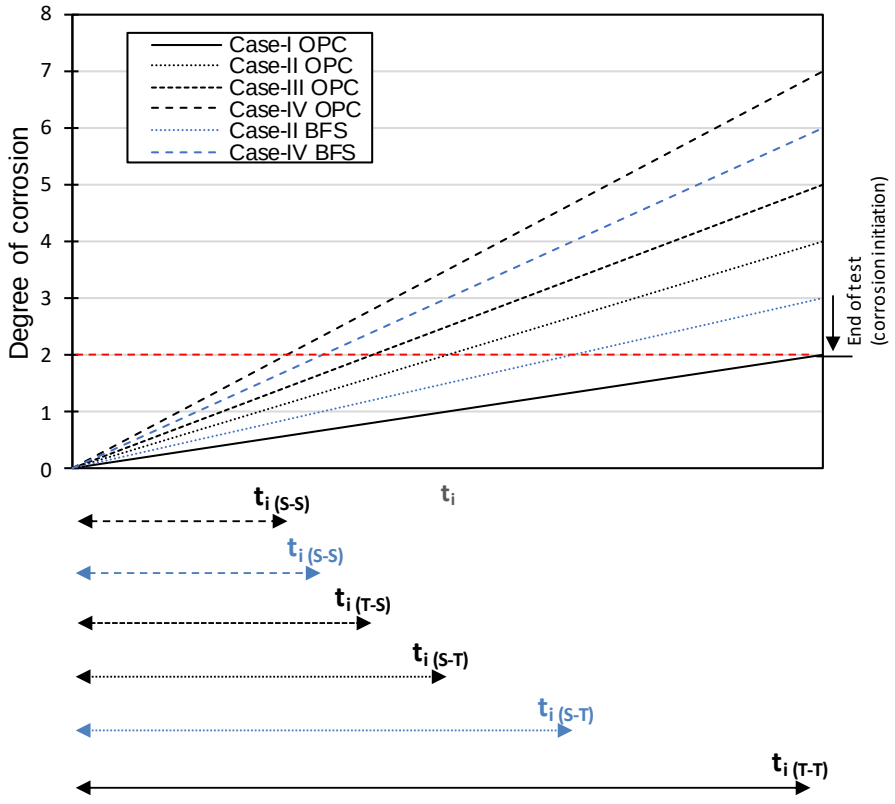

Fig. 18. Estimated time for corrosion initiation due to seawater in concrete

Seawater mixing and curing in Case-IV (S-S) resulted in a HCP more negative than –350 mV in both OPC and GGBFS specimens; further, the HCPs of these specimens

followed a similar trend. However, the anodic-cathodic polarization curves were different. Further, the chloride content in GGBFS specimens was much lower than that in OPC specimens. However, in both specimen sets, chloride content was greater than the threshold value. Unlike in GGBFS specimens, areal corrosion was observed on the steel bar surface in OPC specimens.

The degree of corrosion versus time to corrosion initiation (t_i) due to interaction with seawater is plotted in **Fig. 18**. Case-I (T-T) can be observed to be the most suitable condition with reinforced concrete and tap water for mixing and curing. One interesting point could be noticed in Case-II and Case-III OPC specimens. Case-II specimens needed more time for initiation of corrosion by seawater as compared to Case-III. It can be seen that seawater, when used for curing, influences the degree of corrosion to a much higher extent than when it is used for mixing. Further, SCMs with GGBFS improve the corrosion resistance of concrete to seawater used for mixing (Case-II). The least corrosion resistance could be observed in Case-IV (S-S). However, in unavoidable situations, seawater can be used for mixing and curing under certain conditions. GGBFS (SCMs) can increase the time for corrosion initiation. Accordingly, if proper concrete design is undertaken, seawater can be employed in concrete production. The appropriate concrete design should include 1) a low W/B ratio, 2) an adequate concrete cover, and 3) use of SCMs. In addition, corrosion-resistant bars (i.e., epoxy-coated and stainless steel bars) should be employed in concrete structure exposed to seawater.

5. CONCLUSIONS

Seawater should not be turned down as a mixing and curing agent for concrete, but should be properly applied, especially in coastal areas or distant islands. However, proper handling should be undertaken to avoid concrete failure due to its interaction with seawater. The current study evaluated the applicability of seawater as mixing and curing water and the major conclusions are as follows.

1. Seawater influences the corrosion activity to a greater extent as a curing agent than as a mixing agent.
2. At present study, reported the current compatible for applicability of seawater as mixing and curing water in the following order: Case-I (T-T) > Case-II (S-T) > Case-III (T-S) > Case-IV (S-S).
3. The limitation for seawater application in OPC structures include a maximum W/B ratio of 0.40 and a concrete cover thicker than 50 mm.
4. SCMs provide better corrosion resistance than OPC with seawater as mixing and curing water. In this study, only $GGBFS_{4000}$ is used, therefore future research needs to evaluate the effectiveness of other types of SCMs.
5. It is recommended to use epoxy-coated bars as reinforcement when using seawater for mixing and curing. However, when scratches occur, these bars are vulnerable to corrosion. Future research should concentrate on the effects of such damage on corrosion.

6. Stainless steel bars are the most reliable reinforcement when seawater is used for mixing or curing. However, their life-cycle cost should be considered for optimal process design.
7. In this study, mortar cement specimens were evaluated and in future, research should be undertaken to study the effect of seawater on concrete specimens. Furthermore, the effect of concrete cover thickness should be investigated in detail.

ACKNOWLEDGMENTS

The first author would like to express gratitude to Mr. Masanouri Annoura and Mr. Akira Yakushiji who actively supported this study. The authors wishes to thank the anonymous reviewers for their serious review and constructive comments. The authors also sincerely to thank the editors for their selfless contribution in the manuscript processing.

REFERENCES

[1] A. Neville, Seawater in the mixture, Concr. Int. 23(1) (2001) 48-51.

[2] T. Nishida, N. Otsuki, H. Ohara, M. Garba-Say Zoulkanel, T. Nagata, Some Considerations for Applicability of Seawater as Mixing Water in Concrete, Journal of Materials in Civil Engineering 27(7) (2015) B4014004.

[3] H. Sharon, K.S. Reddy, A review of solar energy driven desalination technologies, Renewable and Sustainable Energy Reviews 41 (2015) 1080-1118.

[4] Standard Specification for Design and Construction of Concrete Structures, Part 2 (Construction), Japan Society of Civil Engineering, Tokyo, Japan, 1986.

[5] Technical Committee on the use of sea water in concrete, Committee Report:JCI-TC121A, Japan Concrete Institute, Tokyo, 2014.

[6] T.U. Mohammed, H. Hamada, T. Yamaji, Performance of seawater-mixed concrete in the tidal environment, Cement and Concrete Research 34(4) (2004) 593-601.

[7] K. Katano, N. Takeda, Y. Ishizeki, K. Iriya, Properties and application of concrete made with sea water and un-washed sea sand, Proceedings of Third International conference on Sustainable Construction Materials and Technologies, 2013.

[8] T. Nishida, N. Otsuki, H. Ohara, Z.M. Garba-Say, T. Nagata, Some considerations for applicability of seawater as mixing water in concrete, Journal of Materials in Civil engineering 27(7) (2013) B4014004.

[9] S.K. Kaushik, S. Islam, Suitability of sea water for mixing structural concrete exposed to a marine environment, Cement and Concrete Composites 17(3) (1995) 177-185.

[10] F.M. Wegian, Effect of seawater for mixing and curing on structural concrete, The IES Journal Part A: Civil & Structural Engineering 3(4) (2010) 235-243.

[11] J. Xiao, C. Qiang, A. Nanni, K. Zhang, Use of sea-sand and seawater in concrete construction: Current status and future opportunities, Construction and Building Materials 155 (2017) 1101-1111.

[12] H.Y. Ghorab, M.S. Hilal, A. Antar, Effect of mixing and curing waters on the behaviour of cement pastes and concrete Part 2: Properties of cement paste and concrete, Cement and

Concrete Research 20(1) (1990) 69-72.

[13] S.D. Ramaswamy, M.A. Aziz, C.K. Murthy, Sea dredged sand for concrete, extending aggregate resources, ASTM Int. 774 (1982) 167-177.

[14] D. Griffin, P. Henry, The effect of salt in concrete on compressive strength, water vapour transmission and corrosion of reinforcing steel, ASTM 63 (1963) 1046.

[15] M. Etxeberria, J.M. Fernandez, J. Limeira, Secondary aggregates and seawater employment for sustainable concrete dyke blocks production: Case study, Construction and Building Materials 113 (2016) 586-595.

[16] D.L. Narver, Good concrete made with coral and water, Civil Engng 24 (1964) 654-658.

[17] N. Otsuki, T. Saito, Y. Tadokoro, Possibility of seawater as mixing water in concrete, Journal of Civil Engineering and Architecture 6(10) (2012) 1273-1279.

[18] R. Shalon, M. Rapheal, Influence of sea water on corrosion of reinforcement, Journal Proceedings, 1959, pp. 1251-1268.

[19] M. Makita, Y. Mori, K. Katawaki, A.C.I. Publication SP-65 (1980) 271-289.

[20] A. Dasar, A STUDY ON DETERIORATION AND CORROSION BEHAVIOR OF RC AND PC MEMBERS WITH INITIAL DEFECTS UNDER ENVIRONMENTAL ACTION, Kyushu University, 2017.

[21] A. Dasar, A Study on Corrosion Evaluation of Steel in Reinforced Concrete due to Chloride Ion, Kyushu University, 2013.

[22] A. Dasar, H. Hamada, Y. Sagawa, R. Irmawaty, Corrosion Evaluation of Reinforcing Bar in Sea Water Mixed Mortar by Electrochemical Method, Proceedings of the Japan Concrete

Institute, Japan Concrete Institute, Nagoya, 2013, pp. 889-894.

[23] A. Dasar, H. Hamada, Y. Sagawa, D. Yamamoto, RECOVERY IN MIX POTENTIAL AND POLARIZATION RESISTANCE OF STEEL BAR IN CEMENT HARDENED MATRIX DURING EARLY AGE OF 6 MONTHS-SEA-WATER MIXED MORTAR AND CRACKED CONCRETE, Proceedings of the Japan Concrete Institute, Japan Concrete Institute, Fukuoka, 2016, pp. 1203-1208.

[24] ASTM, C876-09, Standard Test Method for Corrosion Potentials of Uncoated Reinforcing Steel in Concrete, Philadelphia, US, 2009.

[25] B. Elsener, C. Andrade, J. Gulikers, R. Polder, M. Raupach, Hall-cell potential measurements—Potential mapping on reinforced concrete structures, Materials and Structures 36(7) (2003) 461-471.

[26] N.J. Carino, Nondestructive techniques to investigate corrosion status in concrete structures, Journal of performance of constructed facilities 13(3) (1999) 96-106.

[27] N. Otsuki, A study of effectiveness of chloride on corrosion of steel bar in concrete, Report of Port and Harbor Research Institute (PHRI), Japan (1985) 127-134.

[28] Measurement method for distribution of total chloride ion in concrete structure, Japan Society of Civil Engineering, 2003.

[29] N. Otsuki, Research on the influence of chloride on corrosion of the embedded steel bars in concrete, Rep. of the Port and Harbour Research Institute, Ministry of Transport 24(3) (1985) 183-185.

[30] N.R. Jarrah, O.S.B. Al-Amoudi, M. Maslehuddin, O.A. Ashiru, A.I. Al-Mana,

Electrochemical behaviour of steel in plain and blended cement concretes in sulphate and/or chloride environments, Construction and Building Materials 9(2) (1995) 97-103.

[31] Utilization of blast furnace slag in cement, Nippon Slag Association, 2012, p. 42.

[32] A. Dasar, H. Hamada, Y. Sagawa, T. Ikeda, Durability of Marine Concrete with Mineral Admixture and Marine Aquatic Organism Layer, Sustainable Construction Materials and Technologies 2013 (2013) e146.

[33] JSCE, Standar Specification for Concrete Structures (Part：Design), Japan Society of Civil Engineers, Japan, 2007.

[34] A. Dasar, H. Hamada, Y. Sagawa, D. Yamamoto, Deterioration progress and performance reduction of 40-year-old reinforced concrete beams in natural corrosion environments, Construction and Building Materials 149 (2017) 690-704.

[35] A. Dasar, R. Irmawaty, H. Hamada, Y. Sagawa, D. Yamamoto, Prestress loss and bending capacity of pre-cracked 40 year-old PC beams exposed to marine environment, MATEC Web of Conferences, EDP Sciences, 2016, p. 02008.

[36] J. Gayner, Concrete in hot climates, Precast concrete 10(4) (1979) 169-172.

[37] S. Ozaki, N. Sugata, Sixty-year-old concrete in a marine environment, Special Publication 109 (1988) 587-598.

[38] Recommendations for design and construction of concrete structures using epoxy-coated reinforcing steel bars, Concrete Library 112, Japan Society of Civil Engineers, 2003.

[39] Recommendations for design and construction of concrete structures using stainless steel bars (Draft), Japan Society of Civil Engineers, Japan, 2008.

[40] C.F. Crumpton, B.J. Smith, G. Jayaprakash, Salt weathering of limestone aggregate and concrete without freeze-thaw, Transportation Research Record (1250) (1989).